Article

Not peer-reviewed version

Development of an Immunocapture-Based Polymeric Optical Fiber Sensor for Bacteria Detection

Rafaela Nascimento Lopes , Paulo Henrique Silva Pinto , Juan David Lopez Vargas , Alex Dante , Andrew Macrae , Regina Celia Barros Allil , Marcelo Martins Werneck *

Posted Date: 10 January 2024

doi: 10.20944/preprints202401.0767.v1

Keywords: plastic optical fiber sensor; immunosensor; Escherichia coli; biosensor

Article

Development of an Immunocapture-Based Polymeric Optical Fiber Sensor for Bacteria Detection

Rafaela Nascimento Lopes [1,2], Paulo Henrique Silva Pinto [1], Juan David Lopez Vargas [3], Alex Dante [1], Andrew Macrae [2], Regina Célia Barros Allil [1] and Marcelo Martins Werneck [1,3,*]

[1] Electrical Engineering Program, COPPE, Universidade Federal do Rio de Janeiro, Rio de Janeiro, Brasil
[2] Programa de Pós-graduação em Biotecnologia Vegetal e Bioprocessos, CCS, Universidade Federal do Rio de Janeiro, Rio de Janeiro, Brasil
[3] Nanotecnology Engineering Program, COPPE, Universidade Federal do Rio de Janeiro, Rio de Janeiro, Brasil
* Correspondence: Author, e-mail: werneck@coppe.ufrj.br

Abstract: Conventional methods for pathogen detection in water rely on time-consuming enrichment steps followed by biochemical identification strategies, which require assay times ranging from 24 hours to up to a week. However, in recent years, significant efforts have been made towards the development of biosensing technologies enabling rapid and close-to-real-time detection of waterborne pathogens. In previous studies, we developed a plastic optical fiber (POF) immunosensor using an optoelectronic configuration consisting of a U-Shape probe connected to an LED and a photodetector. Bacterial detection was evaluated with the immunosensor immersed in a bacterial suspension in water with a known concentration. Here, we report on the sensitivity of a new optoelectronic configuration consisting of two POF U-Shape probes, one as the reference and the other as the immunosensor, for the detection of *Escherichia coli*. In addition, another way of detection was tested where the sensors were calibrated in the air, before immersed in bacterial suspension and then read in the air, making the immunosensor more sensitive and with a faster detection time. This new sensor detected the presence of E. coli at 10^4 CFU/mL in less than 10 minutes. Currently sub-10 minutes is faster than previous studies using fiber-optic based biosensors. It is also a much simpler and quicker methodology when compared with conventional laboratory technology.

Keywords: plastic optical fiber sensor; immunosensor; Escherichia coli; biosensor

1. Introduction

Waterborne bacterial, viral and parasitic pathogens are a global health problem. Lack of access to safe drinking water combined with poor hygiene and sanitation facilities, affects more than half of the population in developing countries [1]. About one billion people depend on contaminated water sources, resulting in about 2.2 million deaths annually, mainly caused by diarrheal diseases, which the World Health Organization (WHO) estimates to account for about 4% of the global burden of disease [2].

The detection of pathogens in water is complicated by several obstacles: they are usually present in very low concentrations in the environment and the samples contain numerous inhibitors of enzymatic reactions as well as interfering organisms and particles [2].

Conventional methods for pathogen detection rely on time-consuming enrichment steps followed by biochemical identification strategies that require assay times of 24 hours to one week [3]. In recent years, however, considerable efforts have been made to develop biosensing technologies that enable rapid and near real-time detection of pathogens in water.

A biosensor is a self-contained analytical device consisting of a biological recognition element and a transducer. The analyte, e.g. the bacteria, binds to the biological element, which in turn generates an electronic response in the transducer that can be measured [2]. Optical biosensors using a variety of optical sensing modalities have been promoted as a promising alternative transducer platform for pathogen analysis.

 doi:10.20944/preprints202401.0767.v1

Biosensors can be classified according to the principle of operation under which the transducer works or the type of the bioreceptor. The principle of operation ranges from: a) optical; b) electrochemical; c) mass-sensitive; and d) thermometric. Bioreceptor elements can vary from: a) proteins that catalyze specific chemical reactions; b) antibodies and antigens, based on antibody-antigen interaction in which a specific antibody binds to a specific antigen; c) nucleic acids; d) biomimetic receptors in which recognition is achieved by the use of imprinted polymers that mimic the bioreceptor; and f) whole cells or a specific cellular component [4]. In general, biosensors can detect even minor changes in analytes, enabling sensitive and specific measurements [3].

An example of an electrochemical biosensor can be found in the work of Sobhan et al (2022) [5]. In their research they developed an activated biochar-based immunosensor for the detection of *Escherichia coli* (*E. coli*) cells in pure culture. Biochar is a carbon-rich material produced by decomposition of biomass, such as corn stalks, in the absence of oxygen through a pyrolysis. They immobilized *E. coli* antibodies on the surface of the electrodes and measured the impedance of the immunosensor using an impedance analyzer. They were able to detect a concentration of *E. coli* O157:H7 of only 10^4 CFU/mL.

Biosensors based on antibody-antigen interaction are also known as immunosensors where the biorecognition element is an antibody. Antibodies are biomolecules, or proteins, produced by lymphocytes as a part of the immune system. These types of biosensors are highly selective and can recognize a specific antigen or bacterium among many other species. To function properly, the antibodies are immobilized on the sensor, either on the biochar as we saw above [5] or on the surface of an optical fiber, as we will describe later in this article.

In recent years, optical fibers have been successfully used as immunosensor platforms in various spectral ranges because of their fast response, specificity, sensitivity and low cost. In addition, they are suitable for near real-time monitoring and on-site detection, as shown in Wandermur et al. (2013) [6].

One of the preferred physical parameters of a fiber optic sensor is the refractive index (RI), which changes depending on the external environment and can be used as a sensing basis, but many studies present different parameters used for detection, as described by Wang and Wolbeis (2020) [7], who provide an overview of these sensors.

For example, Razo-Medina et al. (2018) [8] have described a biosensor for cholesterol based on a thin film of a cholesterol enzyme encapsulated in a sol-gel film applied to the end of a plastic optical fiber.

In a fiber-optic biosensor, the immobilization of the enzymes on the fiber surface is normally achieved by chemical modification. In the article of Li et al (2021) [9], they used electrospinning to immobilize the enzyme on the optical fiber sensor for the detection of glucose.

These are many examples that show different techniques applying optical fiber sensors; for a more detailed description of these methodologies, it is worth to read the article of Leitão et al (2022) [10]. The paper describes cost-effective fiber configurations such as end-face, reflected, uncladded, D-shape, U-shape, tips, tapered, amongst others.

Another way to apply an optical fiber as a sensor is based on the surface plasmon resonance (SPR) phenomena. Traditional SPR systems use a thin metal film deposited on the surface of a prism. An incident light excites the free conduction electrons at the interface between the metal and a dielectric and is reflected by the prism. A monochromator measures the intensity and wavelength of the reflected light at the thin metal film. The light is more attenuated (absorbed by the electrons resonance) at a specific angle and a specific wavelength that depends on the metal film used. Many factors can change the wavelength, such as refractive index of a liquid in contact with the thin film or the presence of molecules attached to the film [11].

Since the late 1970's SPR was believed to be useful to characterize thin films or to monitor chemical process occurring over the thin film and Nylander et al (1982) [12] were the first to apply SPR for gas detection and biosensing.

Later, Mitsushio et al. (2006) [13] deposited 45-nm thin films of Au, Ag, Cu, and Al on the surface of an optical fiber and thus developed an SPR-based optical fiber sensor for the first time. After this

first application, many articles have been published with a variety of sensing applications, such as Arcas et al (2018) [14], detected *E. coli* with a U-shape plastic optical fiber covered with an Au nanofilm, Arcas et al. (2021) [15] detected *Taenia solium*, the pork tapeworm that causes intestinal infection after eating contaminated pork, Cennano et al. (2021) [16] detected SARS-CoV-2 with an SPR-based optical fiber sensor, and Alberti et al. (2022) [17] detected uranium in water.

Plastic optical fibers (POF) were first developed by DuPont in 1963. They were made of polystyrene and had losses in the range of 500 to 1000 dB/km. They were initially used for lighting over short distances. Today, we use conventional POFs made of polymethyl methacrylate (PMMA), which were also developed by DuPont in 1968, with losses in the range of 300 dB/km [18].

Contrary to the silica fibers, since their first applications, POFs did not evolve much in transmission losses. Just for comparison, the ESKA® PMMA fiber from Mitsubishi Rayon presents an attenuation value of 180 dB/km at 650 nm. With this so large attenuation, POFs found applications mainly for short-distance telecom, such as 100 m, but at the same time POFs attracted attention for sensor development. The reason for this is that POFs can be connected to readily available transmission components at low cost by using simple tools as will be seen in this paper.

POFs have additional advantages of high strain limit, high durability, and negative thermo-optic coefficients. With these unique properties, POFs have been applied in various sensors applications, such as chemical/biological and radiation sensing as well as those of strain, temperature, and displacement.

There are many books available on optical fiber sensors, however just a few deals specifically with plastic optical fiber sensors, possibly because POF sensors are relatively new in the optical fiber sensing area. POF sensors are much easier to design, mainly because the unique POF characteristics, such as easy handling, large diameter, cheap peripheral components, and simple tools [18].

Plastic optical fiber sensors have been the focus of research in our lab because they offer numerous advantages over silica fibers, including a larger diameter that facilitates handling, good light coupling, and the use of low-cost peripheral components such as LEDs and photodetectors. One of our first studies was conducted by Beres et al. (2011) [19] on the detection of *E. coli* in water using a tapered POF sensor. Subsequently, Wandermur et al. (2014) [6] developed a U-Shape POF sensor in an electronic platform for the rapid detection of bacteria. Following these studies, Rodrigues et al. (2017) [20] investigated the sensitivity of different forms of a U-Shape POF sensor and searched for better efficiency at low bacterial dilution, while Lopes et al. (2018) [21] used a specific U-Shape sensor format for the detection of sulfate-reducing bacteria, such as *Desulfovibrio alaskensis*, which are found in crude oil and are responsible for the production of hydrogen sulfite (H_2S), which reacts in the presence of water and produces sulfuric acid (H_2SO_4) that corrodes the steel of the pipelines.

Many other studies in which POF sensors were used are available, such as the work by Ashraf et al. (2022) [22], in which a U-Shape POF was used for the detection of iron supplements, and in another work by Ashraf et al. (2023) [23], a U-Shape POF was used for the detection of phosphate in water.

Also worth mentioning is the work of Johari et al. (2022) [24], who used a tapered U-Shape POF sensor coated with ZnO nanorods to measure relative humidity, and the work of Hadi and Khurshid (2022) [25], who used a U-Shape POF immunosensor for the detection of SARS-CoV-2.

The above-mentioned U-Shape POF sensors use one of the most common operating principles of POF immunosensors, that is the change in guided light output at the fiber end in response to the pathogens captured by the immobilized antibodies on the fiber surface. In previous studies, we have developed a POF immunosensor using an optoelectronic configuration consisting of a U-Shape probe connected to an 880 nm LED and a photodetector [21], [26].

In this article, we report a new development in which we used a new reading method and an improved electronic system consisting of two POF U-Shape probes, one as a reference and the other as an immunosensor. We evaluate the sensitivity of this novel optoelectronic configuration for the detection of *E. coli*.

Preprints (www.preprints.org) | NOT PEER-REVIEWED | Posted: 10 January 2024 doi:10.20944/preprints202401.0767.v1

2. Sensing Theory: Physical Principle of a U-Shape POF Sensor

This section explains the mechanism by which the developed immunosensor works and the theories associated with this sensing method. The sensor is based on the change in the refractive index (RI) within the evanescent wave created near the fiber surface by the bacteria captured through the antigen-antibody effect.

Figure 1 shows a schematic representation of the sensing principle using a U-Shape POF sensor immersed in a liquid containing several species of bacteria. A near-infrared LED is used to couple light into an uncladded poly (methyl methacrylate) (PMMA) fiber, and the light is transmitted through the fiber. A microcontroller controls the optical output power of the LED, which is coupled into the sensor. The light is guided through the fiber to the photodetector, which converts the light into photocurrent, which is then converted into voltage levels that are properly conditioned and detected by the microcontroller. The fiber surface is functionalized with a specific antibody that performs the immunocapture process, specifically for *E. coli* bacteria. As bacteria are attracted and captured on the fiber surface, the RI of the interface between the fiber core and the outer medium changes, which in turn changes the guiding conditions of the fiber. As a result, the optical output power at the fiber end varies depending on the number of bacteria captured by the antibody.

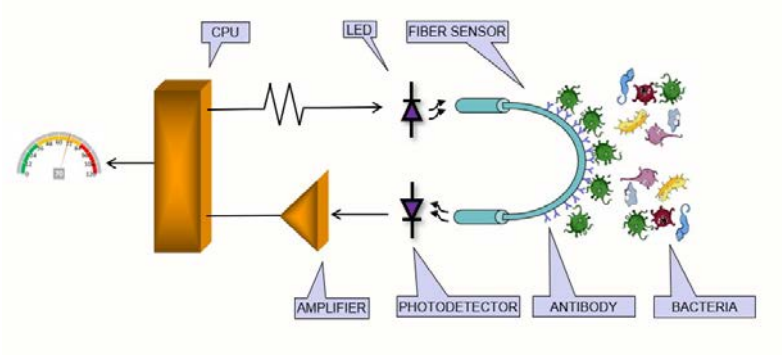

Figure 1. Schematic diagram of the sensing system. A CPU controls the LED output power that is coupled into the POF U-Shape. The light is guided by the fiber to the photodetector, which output returns to the microcontroller. The fiber surface is functionalized with a specific antibody that performs the immunocapture process, specifically for E. coli.

3. Materials e Methods

3.1. Manufacture of U-Shape Sensors

The POF used to manufacture the proposed immunosensor has a core diameter of 980 µm with a 10 µm cladding, made of poly (methyl methacrylate) (PMMA) (Mitsubishi model CK40 Eska®). In previous studies, we observed that the fiber cladding prevented a good functionalization and immobilization of the antibodies on its surface because it is made of PMMA and other polymers that renders the RI below that of the core [21]. Therefore, we removed the 10-µm thick cladding by the following procedure: the curve of the sensor was placed inside the folding of an optical cleaning tissue, applied 50 µL of acetone and the fiber curve is gently hand-rubbed. After that, the sensor was rinsed in distilled water to neutralize the effect of corrosion [20].

For the sensor fabrication, the fiber was cleaved into 10-cm long sections and both end surfaces were polished by a 1,500-grit sandpaper for a better light coupling. Following that, the fiber sections were rinsed with deionized water and blow-dried with nitrogen. Then, the POFs were bent around a 10-mm width 3-D printed mold to produce the U-Shape probes, and heated in an oven at 70° C. The sensors were tested under different RI, to check for reproducibility and to calibrate their sensitivity, and further functionalized with antibodies. Twenty sensors were fabricated to produce 10 reference sensors and 10 immunosensors. Five pairs were used to detect bacteria in a 10^8 CFU/mL (Colony Forming Unities per milliliter) suspension and the other five pairs were used to detect 10^4 CFU/mL suspension.

 doi:10.20944/preprints202401.0767.v1

3.2. Sensor Surface Functionalization with Polyethyleneimine (PEI) and Immobilization of Antibodies

The following protocol modified from [27] was adopted to functionalize the probes: The sensors were treated with sulfuric acid (H_2SO_4) solution 3:1 for 2 hours at 60° C. After being washed with ultrapure water, the sensors were incubated in a 2% PEI solution in dimethyl sulfoxide (DMSO) (Sigma-Aldrich, USA) for 24 hours at room temperature. For crosslinking the amino group and fixing the antibodies, the sensors were incubated in a 2.5% glutaraldehyde (Sigma-Aldrich, USA) solution in pH 7.0 phosphate buffer for 24 hours at 37° C. Then, the sensors were washed in phosphate buffer pH 7.0 and dried overnight at 30° C.

The next step was the fixation of antibody to the amine radicals immobilized earlier on the fiber surface. The sensors were incubated with protein A (Sigma-Aldrich, St. Louis, USA) for one hour at 30 °C, followed by incubation for four hours in a solution of 0.1 mg/mL of anti-*E. coli* antibodies (Bio-Rad, UK).

3.3. Bacteria Suspension and E. coli Detection Procedures

E. coli O55 bacterial strains were used to prepare the suspensions that were cultivated in Tryptic Soy Agar (Merck, Darmstadt, Germany) and incubated for 24 hours at 37°C. Subsequently, bacterial suspensions were prepared by adding growth colonies into a tube containing 10 mL of 0.85% saline solution. The tube was vortexed for homogenization and compared to the turbidity of the McFarland scale 0.5, equivalent to 10^8 CFU/mL. In the other tubes 9 mL of 0.85% saline solution were added to prepare suspensions diluted to 10^4 CFU/mL by adding 1 mL of the previously diluted solution.

For bacterial detection, we prepared five beakers with 10^8 CFU/mL suspension and other five beakers with 10^4 CFU/mL suspension to produce five response curves for the 10^8 CFU/mL and five response curves for the 10^4 CFU/mL.

3.4. The Optoelectronic System

Figure 2 shows the block diagram of the developed electronic instrumentation. The sensing head employed for housing the reference sensor and immunosensor was fabricated in aluminum. It accommodates both the input and output ends of U-Shape POFs, one functionalized with antibodies for bacteria detection, as described on the previous section, and another one not functionalized, to be used as a reference sensor. The use of a single LED as the light source for both U-Shape POF sensors compensates for eventual optical power fluctuations.

The output signal from the two photodetectors employed were connected to low-noise FET-input op-amps arranged as transimpedance amplifiers (TL072, Texas Instruments Inc.) providing two voltage outputs, one as the reference, and the other as the sensing signal itself. Each signal was connected to the inputs of an instrumentation amplifier (INA121, Texas Instruments Inc.) that performs a differential measurement, and the output signal was then filtered and sampled by a 16-bit resolution analog-to-digital converter (DAQ USB-6002, National Instruments Inc.). From a 16-bit digital-to-analog converter also available in the DAQ, a current source was implemented to control the LED.

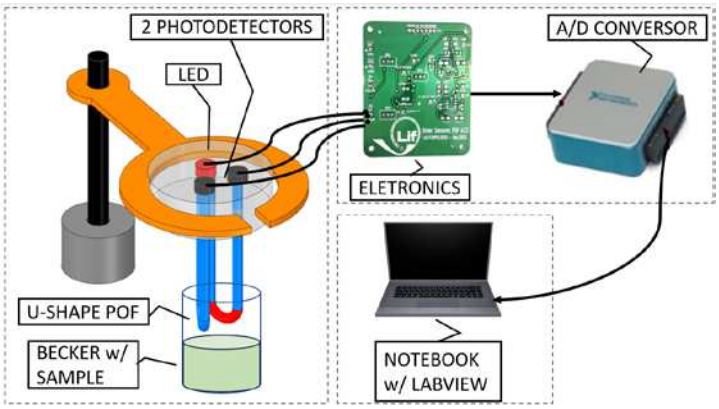

Preprints (www.preprints.org) | NOT PEER-REVIEWED | Posted: 10 January 2024 doi:10.20944/preprints202401.0767.v1

Figure 2. Optoelectronic setup developed for the immunosensor for sensing, signal acquisition and conditioning.

A dedicated Graphical User Interface (GUI) was built in LabVIEW to support the optoelectronic instrumentation. Figure 3 shows the front panel view of the developed software.

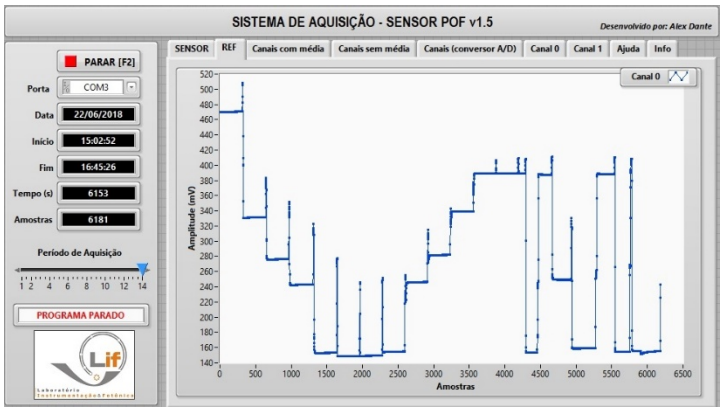

Figure 3. Front panel view of the software showing the response of one U-Shape sensor when immersed in water with different refractive indices (1.33, 1.35, 1.36, 1.37, 1.38, 1.39). The idea of this test was to check the stability and repeatability of the measurements.

3.5. Measurement Methodology

When bacteria in the water adhere to the fiber surface, the RI of the surrounding media changes from 1.33 (pure water) to something below 1.39 (pure bacteria). Measuring the effect of this small RI variation on the sensor output light needed an extremely high gain with a very high signal-to-noise ratio, using the methodology applied previously [6]. To circumvent the small difference in the output voltage of the electronic system, a new methodology was tested to generate larger differences between sensors with bacteria and sensors without bacteria. If the sensors were read outside the water, in contact with the air, the presence of bacteria along the fiber surface containing patches of 1.39 refractive indices, contrast better with a RI=1 (air) than with a RI=1.33 (water). Therefore, the sensing methodology adopted, shown in Figure 4 is: A) Calibration of the reference sensor and the immunosensor in air (RI=1); B) Both sensors are immersed in the *E. coli* suspension for 10 minutes; C) Sensors are suspended from the beaker to the air and read again by the system.

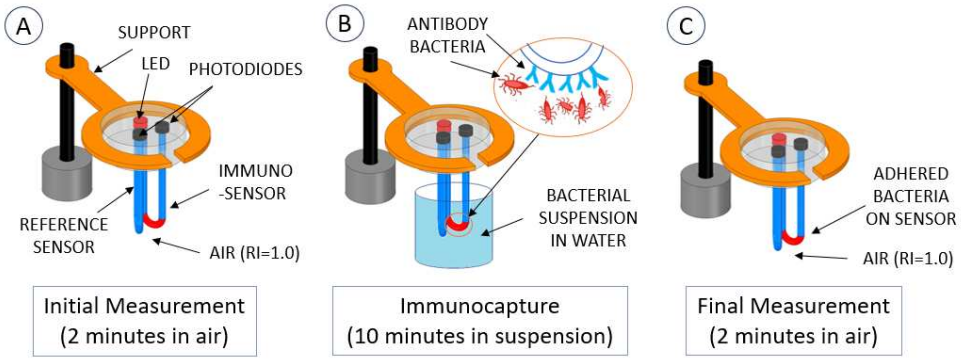

Figure 4. Measurement procedure for bacteria detection.

3.6. Test and Simulation of the Methodology

To verify that the sensor method provides real results, a confirmation test was performed with the following methodology: Two U-Shape sensors, an uncladded POF as a reference and a conventional pristine cladded POF simulating the presence of bacteria around the fiber, were inserted, and removed from a beaker containing pure water. The results of this test are shown in Section 4.

Preprints (www.preprints.org) | NOT PEER-REVIEWED | Posted: 10 January 2024 doi:10.20944/preprints202401.0767.v1

4. Results

4.1. Results of Immunocapture

After all functionalization processes and RI measurements four sensor pairs were used to detect *E. coli* at 10^8 CFU/mL and other four sensor pairs at o 10^4 CFU/mL. Figure 5 and Figure 6 show respectively the result of four sensors in 10^8 CFU/mL and four sensors in 10^4 CFU/mL. Notice that, in both cases, the reference sensor output returns to the same level it was before immersion in the analyte, as expected, whereas the immunosensor shows a higher level after immersion due to the bacteria adhered to its surface.

The results for all sensors were essentially similar, with the immunosensor presenting a higher output after detection, however, due to the larger number of bacteria adhered to the sensor in the 10^8 CFU/mL analyte, the output power was higher because more light was transmitted by the fiber, than in the 10^4 CFU/mL analyte. This behavior at both bacterial concentrations was expected because the surrounding bacteria around the fiber acts as a fiber core, allowing the fiber to transmit more propagation modes than in the other case.

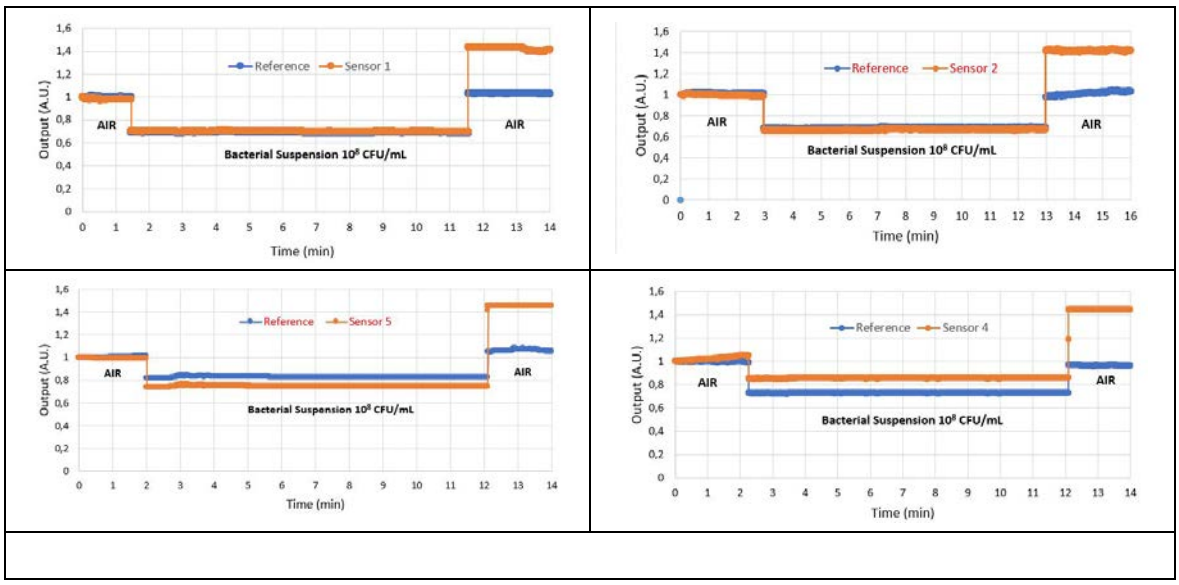

Figure 5. Results of four sensors in the detection of *E. coli* in bacterial suspension of 10^8 CFU/mL.

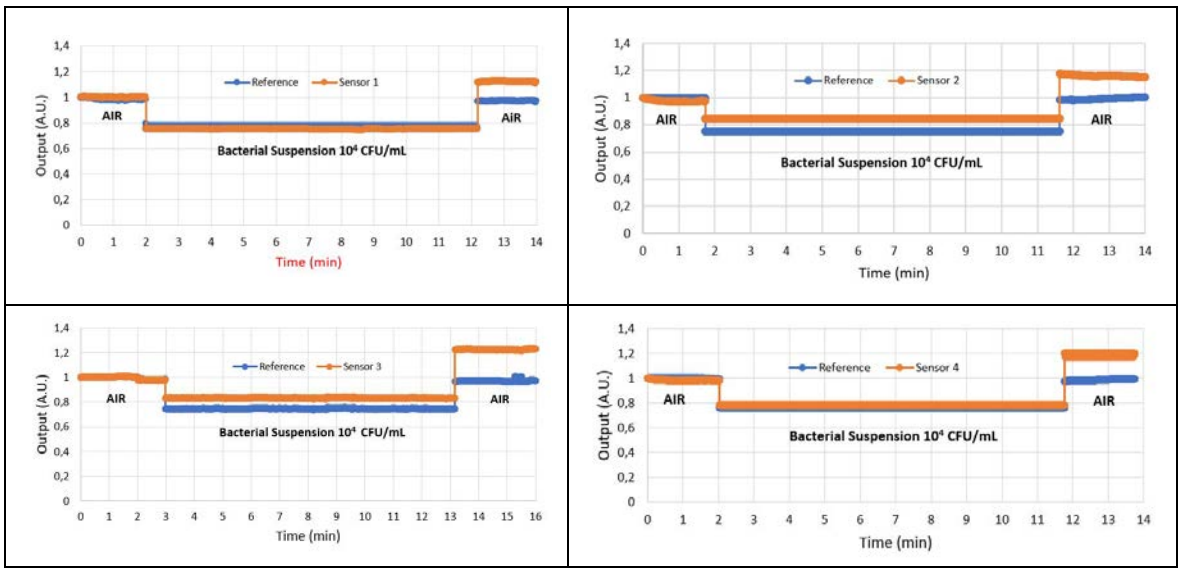

Figure 6. Results of four sensors in the detection of *E. coli* in bacterial suspension of 10^4 CFU/mL.4.2. Results of Simulation of Immunosensor Behavior.

Preprints (www.preprints.org) | NOT PEER-REVIEWED | Posted: 10 January 2024 doi:10.20944/preprints202401.0767.v1

Two U-Shape sensors, an uncladded POF as a reference and a conventional pristine cladded POF, simulating the immunosensor after bacterial adhesion, were tested in the system. The PMMA fiber core has an RI of 1.49 and the fluorinated polymer cladding has an RI of about 1.40. The two U-Shape sensors were illuminated with the same LED in the circuit shown in Figure 2 and placed in a beaker of pure water, then exposed to air and then immersed in water again.

Due to the fiber curvature in a diameter of 10 mm, the two sensors lose light, both in water and in the air. In water, the two sensors produced approximately the same output power, since the outer RI of the uncladded fiber is 1.33 (water), while the outer RI of the original fiber is 1.40 (the RI of the cladding). When both sensors were brought out of the water into the air, the outer RI of the uncladded sensor changed to 1, while the outer RI of the cladded sensor remained unchanged. However, the cladded fiber increased its light conductivity more than the uncladded sensor due to the air outside the cladding. Consequently, the cladded fiber had a higher output power than the uncladded sensor. With this analogy, it is possible to validate the behavior of the immunosensor after the detection of bacteria. The results of this test are shown in Figure 7.

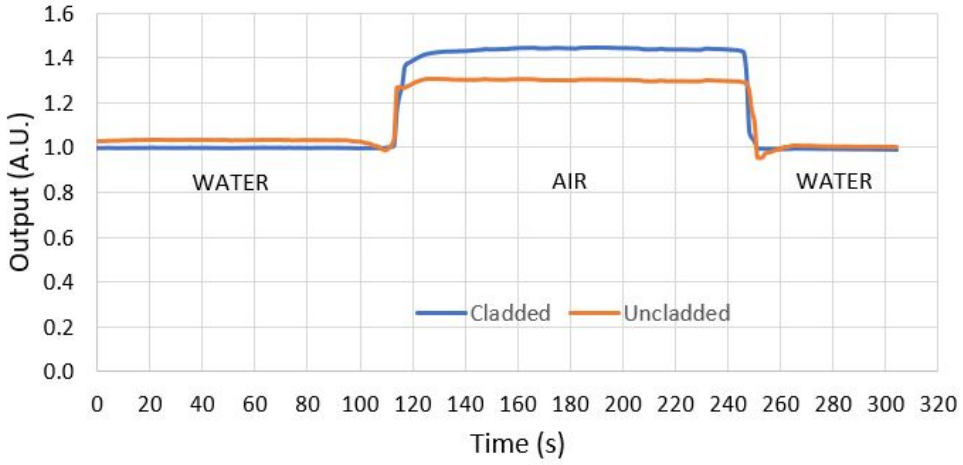

Figure 7. Results of the simulation test with two U-Shape sensors, an uncladded POF as a reference and a conventional pristine cladded POF simulating the immunosensor after bacteria adhesion. The cladded fiber increased its guiding capability more than the uncladded fiber due to the air outside the cladding, and therefore showed a higher output power than the uncladded fiber.

4.3. Tests of Fluorescence in Confocal Microscope

After functionalization with PEI, immobilization of the anti-*E. coli* antibodies and immunocapture for 10 minutes in the bacterial suspension, the immunosensors were washed in PBS 1x (phosphate buffer saline), immersed in DAPI solution for 10 minutes and submitted to confocal microscopy (Leica CTR 4000).

Figure 8 shows the micrograph and histogram of DAPI-stained 1 mm U-Shape POF immunosensors after immunocapture of *E. coli* in bacterial suspension of 10^8 UFC/mL. An area of approximately 1.6 x 10^5 μm^2 was analyzed with a total average volume of 50.81 gray values.

Preprints (www.preprints.org) | NOT PEER-REVIEWED | Posted: 10 January 2024 doi:10.20944/preprints202401.0767.v1

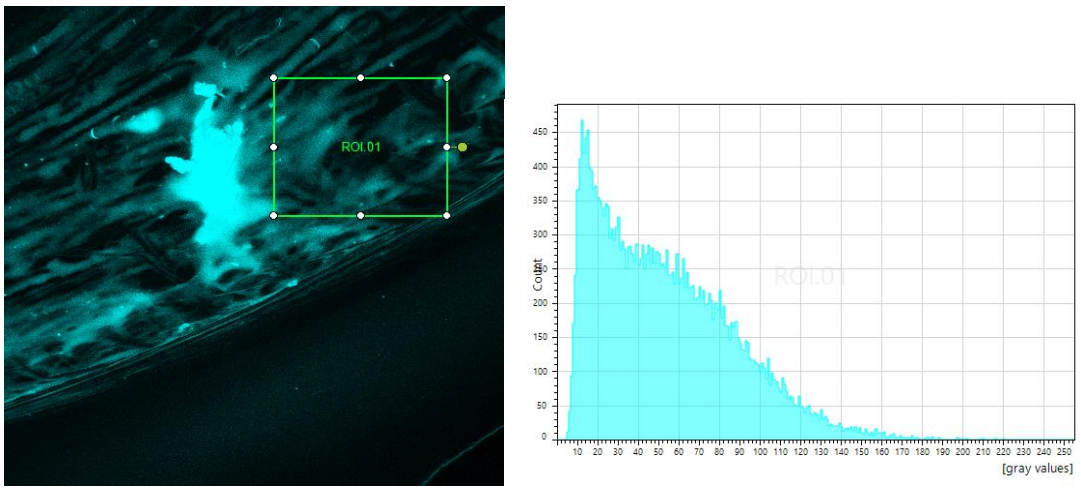

Figure 8. (Left) Micrograph of a 3D reconstruction of DAPI-labeled POF immunosensor after 10 minutes in bacterial suspension of 10^8 CFU/mL. The inserted square represents the area of 1.6 x 10^5 µm² at 10x magnification, submitted to the evaluation of fluorescence intensity. (Right) Graph of the fluorescence intensity distribution of the evaluated area.

Figure 9 shows the micrograph and histogram of DAPI-stained 1 mm U-Shape POF immunosensors after immunocapture of *E. coli* in bacterial suspension of 10^4 UFC/mL. An area of approximately 1.6 x 10^5 µm² was analyzed with a total average volume of 10.35 gray values.

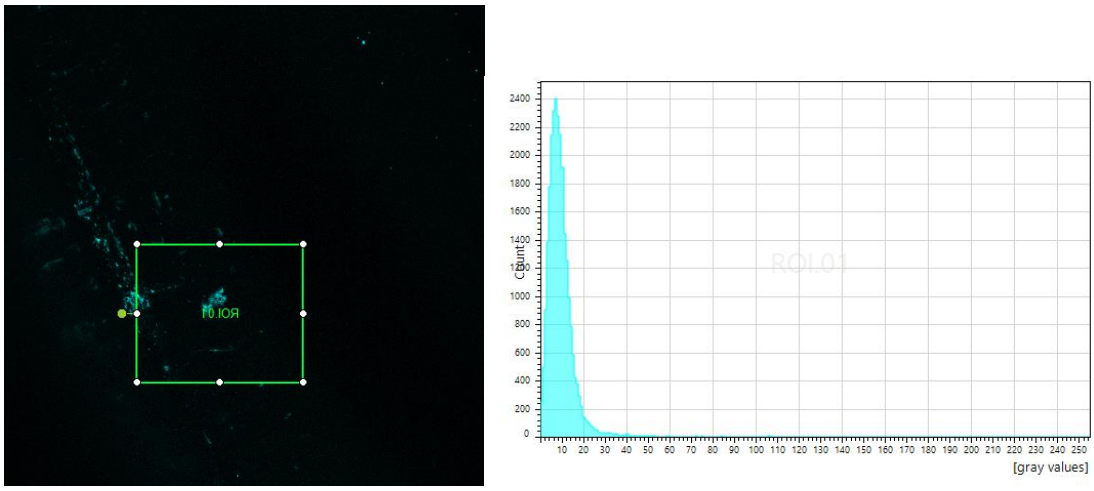

Figure 9. (Left) Micrograph of a 3D reconstruction of DAPI-labeled POF immunosensor after 10 minutes in bacterial suspension of 10^4 CFU/mL. The inserted square represents the area of 1.6 x 10^5 µm² at 10x magnification, submitted to the evaluation of fluorescence intensity. (Right) Graph of the fluorescence intensity distribution of the evaluated area.

The histograms presented show that the immunosensor captured the bacteria confirming that the increase in the output power of the immunosensor was due to the presence of bacteria. Additionally, it is possible to notice from the histograms that the number of captured bacteria is higher for the 10^8 UFC/mL concentration than for 10^4 UFC/mL concentration.

The increase in the output power observed in response to *E. coli* detection in air was because the bacteria captured by the antibody acts as a new fiber cladding, which guides the light inside the fiber, in contrast with the reference sensor, which is without a bacterial cladding.

Although bacterial concentrations found in real-world samples, such as in the water potability assessments, can range in a much smaller concentrations (typically from 10^2 to 10^1 CFU/mL) than those tested in this work, the results obtained show that the immunosensor and measurement methodology proposed here could be developed to detect *E. coli* in in suspension at concentrations

lower than 10^4 CFU/mL. This is an important goal that is currently being assessed by our group through improvements in the proposed immunosensor's sensitivity, as well as in the optoelectronic system to allow for the detection of bacteria at lower concentrations. One of the improvements that will be implemented, for instance, is based on different sensor shapes, as already demonstrated in a recent study [28]. It is important to note, however, that the detection of lower concentrations is also limited by the sensitivity of the antibody provided by the manufacturer.

5. Discussion and Conclusions

As already mentioned, plastic optical fibers were first developed by DuPont in 1963 and used for short-distance illumination [18]. Due to transmission losses, they were soon replaced by silica fibers and the focus of POF application shifted to sensor development. POFs can be easily connected to readily available transmission components, resulting in low-cost devices. Due to these unique properties, POFs have been used in various sensing applications, such as physical, chemical and biological sensing, as well as strain, temperature and displacement measurement. The pioneering study by Beres et al. (2011) [19] on the detection of *E. coli* in water using a tapered POF sensor was taken to a new level in this study by not only detecting but also quantifying *E. coli*. Subsequently, Wandermur et al. (2014) [6] developed a U-Shape POF sensor in an electronic platform for the rapid detection of bacteria. Following these studies, Rodrigues et al. (2017) [20] investigated the sensitivity of different forms of a U-Shape POF sensor and searched for better efficiency at low bacterial dilution, while Lopes et al. (2018) [21] used a specific U-Shape sensor format for the detection of sulfate-reducing bacteria, such as *Desulfovibrio alaskensis*. In this paper we reinforce the use of POFs for the detection of specific bacterial species and the open the door to quantifying them.

The experimental results showed that the responses of the sensor sets were repetitive, confirming the good stability of both the immunosensors and the proposed measurement method. Moreover, the histograms of the fluorescence intensity distribution of the sensor surface confirm the results obtained by the immunosensors and show that the sensor has de facto captured bacteria that caused the observed increase in the output signals.

The new method of reading the sensor outside the water has shown better performance than the method presented in previous work where the sensors were read inside the water. The reason for this is that outside the water the external RI is 1 (air), which makes a greater difference to the RI of the adhering bacteria than inside the water, where the external RI is 1.33, which is very close to that of the bacteria.

When comparing the present sensor system to others with similar sensitivity, response time and detection limit, the main advantages are the simplicity of the system, the manufacturing costs and the size, which allow easy transportation to the site of use.

This new POF-based immunosensor was able to detect the presence of *E. coli* at a concentration of 10^4 CFU/mL within 10 minutes. This new method sets a new standard in sensitivity and is currently the fastest *E. coli* biosensor available and a significant improvement over conventional laboratory detection technology.

One of the next steps our group is currently considering is to improve the sensitivity of the sensor to enable the detection of bacteria at lower concentrations. One of the improvements to be realized, for example, is based on different sensor shapes, as already shown in a recent study [28].

Author Contributions: Investigation, R.N.L.; hardware and software, A.D. and P.H.S.P.; validation, J.D.L.V.; supervision, M.M.W, R.C.B.A. and A.M. All authors have read and agreed to the published version of the manuscript.

Funding: This study was financed in part by the Coordenação de Aperfeiçoamento de Pessoal de Nível Superior—Brasil (CAPES) Finance Code 001.

References

1. Conelly: J.T.; Baeumner, A.J. Biosensor for the Detection of Waterborne Pathogens. *Analytical and Bioanalytical Chemistry*, v. 402, p. 117-127, 2012.
2. Deshmukh, R.A.; Joshi, K.; Bhand, S.; Roy, U. Recent Developments in Detection and Enumeration of Waterborne Bacteria: a Retrospective Minireview. *Microbiology Open*. v. 5(6), p. 901-922, 2016.
3. N. Kumar, Y. Hu, S. Singh, B. Mizaikoff, *"Emerging Biosensor Platforms for the Assessment of Water-borne Pathogens"*, Analyst, 143, 359-373, 2018.
4. María Dolores Marazuela and María Cruz Moreno-Bondi, "Fiber-optic biosensors – an overview". Anal Bioanal Chem (2002) 372 :664–682. doi: 10.1007/s00216-002-1235-9.
5. Sobhan, A.; Jia, F.; Kelso, L.C.; Biswas, S.K.; Muthukumarappan, K.; Cao, C.; Wei, L.; Li, Y. A Novel Activated Biochar-Based Immunosensor for Rapid Detection of E. coli O157:H7. Biosensors 2022, 12, 908. doi: 10.3390/bios12100908
6. Gisele Wandermur, Domingos Rodrigues, Regina Allil, Vanessa Queiroz, Raquel Peixoto, Marcelo Werneck, Marco Miguel, "Plastic optical fiber-based biosensor platform for rapid cell detection". Biosensors and Bioelectronics, Volume 54, 2014, Pages 661-666, ISSN 0956-5663. DOI: https://doi.org/10.1016/j.bios.2013.11.030
7. Xu-dong Wang, and Otto S. Wolfbeis, "Fiber-Optic Chemical Sensors and Biosensors (2015−2019)". Anal. Chem. 2020, 92, 397−430. doi: 10.1021/acs.analchem.9b04708
8. Razo-Medina, D. A., M. Trejo-Durán, and E. Alvarado-Méndez. "Cholesterol Biosensor Based on a Plastic Optical Fibre with Sol-gel: Structural Analysis and Sensing Properties." Journal of Modern Optics 65.3 (2018): 348-52. DOI: https://doi.org/10.1080/09500340.2017.1397223
9. Jinze Li, Xin Liu, Hao Sun, Liming Wang, Jianqi Zhang, Xi Huang, Li Deng, Jiawei Xi, and Tianhong Ma. "A New Type of Optical Fiber Glucose Biosensor With Enzyme Immobilized by Electrospinning." IEEE Sensors Journal 21.14 (2021): 16078-6085. doi: 10.1109/JSEN.2021.3075553
10. Cátia Leitão, Sónia O. Pereira, Carlos Marques , Nunzio Cennamo, Luigi Zeni, Madina Shaimerdenova, Takhmina Ayupova and Daniele Tosi, "Cost-Effective Fiber Optic Solutions for Biosensing". Biosensors 2022, 12, 575. doi: 10.3390/bios12080575
11. Jiří Homola, Sinclair S. Yee, Günter Gauglitz, "Surface plasmon resonance sensors: review". Sensors and Actuators B: Chemical, Volume 54, Issues 1–2, 1999, Pages 3-15, ISSN 0925-4005. doi: 10.1016/S0925-4005(98)00321-9
12. Claes Nylander, Bo Liedberg, Tommy Lind, "Gas detection by means of surface plasmon resonance". Sensors and Actuators, Volume 3, 1982, Pages 79-88, ISSN 0250-6874. doi: 10.1016/0250-6874(82)80008-5
13. Masaru Mitsushio, Kenichiro Miyashita, Morihide Higo, "Sensor properties and surface characterization of the metal-deposited SPR optical fiber sensors with Au, Ag, Cu, and Al". Sensors and Actuators A: Physical, Volume 125, Issue 2, 2006, Pages 296-303, ISSN 0924-4247. doi: 10.1016/j.sna.2005.08.019
14. Arcas, A.D.S.; Dutra, F.D.S.; Allil, R.C.S.B.; Werneck, M.M. Surface Plasmon Resonance and Bending Loss-Based U-Shaped Plastic Optical Fiber Biosensors. Sensors, 2018, 18, 648. doi: 10.3390/s18020648
15. Ariadny S. Arcas, Lizeth Jaramillo, Natalia S. Costa, Regina Celia S. B. Allil, and Marcelo M. Werneck, "Localized surface plasmon resonance-based biosensor on gold nanoparticles for Taenia solium detection". Applied Optics, September, 2021, doi: 10.1364/AO.432990
16. Nunzio Cennamo, Girolamo D'Agostino, Chiara Perri, Francesco Arcadio, Guido Chiaretti, Eva Maria Parisio, Giulio Camarlinghi, Chiara Vettori, Francesco Di Marzo, Rosario Cennamo, Giovanni Porto and Luigi Zeni, "Proof of concept for a quick and highly sensitive on-site detection of SARS-CoV-2 by plasmonic optical fibers and molecularly imprinted polymers". Sensors 2021, 21, 1681. doi: 10.3390/s21051681
17. Alberti, G.; Pesavento, M.; De Maria, L.; Cennamo, N.; Zeni, L.; Merli, D. An Optical Fiber Sensor for Uranium Detection in Water. Biosensors 2022, 12, 635. doi: 10.3390/bios12080635
18. Werneck, M.M., & Allil, R.C.S.B. (Eds.). (2019). Plastic Optical Fiber Sensors: Science, Technology and Applications (1st ed.). CRC Press. https://doi.org/10.1201/b22357
19. Carolina Beres, Fábio Vieira Batista de Nazaré, Nathália Correa Chagas de Souza, Marco Antônio Lemos Miguel, Marcelo Martins Werneck. "Tapered plastic optical fiber-based biosensor – Tests and application". Biosensors and Bioelectronics, Volume 30, Issue 1, 2011, Pages 328-332, ISSN 0956-5663. doi: 10.1016/j.bios.2011.09.024

20. D.M.C. Rodrigues, R.N. Lopes, M.A.R. Franco, R.C.S.B. Allil, M.M. Werneck, “Sensitivity Analysis of Different Shapes of a Plastic Optical Fiber-Based Immunosensor for Escherichia coli: Simulation and Experimental Results”, Sensors, 17 (2944), 1-16, 2017. doi: 10.3390/s17122944.
21. R.N. Lopes, D.M.C. Rodrigues, R.C.S. Allil, M.M. Werneck, “Plastic optical fiber immunosensor for fast detection of sulfate-reducing bacteria”, Measurement, Volume 125, September 2018, Pages 377-385. doi:10.1016/j.measurement.2018.04.088
22. Ashraf, Mainuddin, M. T. Beg, F. Moin, R. Rajesh and G. Singhal, "U-Bent Plastic Optical Fiber Sensor for Iron in Iron Supplements," in IEEE Sensors Journal, vol. 22, no. 15, pp. 14921-14928, 1 Aug.1, 2022. doi: 10.1109/JSEN.2022.3187829
23. Ashraf, Mohd & Siddique, Mainuddin & Beg, Mirza & Moin, Fiza & Saikia, Ananta & Dwivedi, Sanjai & Kumar, Gagan. (2023). U-shaped plastic optical fiber sensor for phosphate detection in water. Optical and Quantum Electronics. doi: 10.1007/s11082-023-05466-5
24. Johari, S.H.; Cheak, T.Z.; Abdul Rahim, H.R.; Jali, M.H.; Mohd Yusof, H.H.; Md Johari, M.A.; Yasin, M.; Harun, S.W. ZnO Nanorods Coated Tapered U-Shape Plastic Optical Fiber for Relative Humidity Detection. Photonics 2022, 9, 796. doi: 10.3390/photonics9110796
25. Hadi, M.U.; Khurshid, M. SARS-CoV-2 Detection Using Optical Fiber Based Sensor Method. Sensors 2022, 22, 751. doi: 10.3390/s22030751
26. Ariadny Da Silva Arcas, Regina Célia Da Silva Barros Allil and Marcelo Martins Werneck, “U-Shaped POF sensor coated with gold thin film for E. coli detection”, Paper 56, Proceedings of the 26th International Conference on Plastic Optical Fibres, POF2017, held at Melia Ria Hotel & Spa, Aveiro, Portugal, ISBN: 978-989-97345-2-4, September 13 to 15, 2017.
27. Khnouf, R; Karasneh, D; Albiss, B.A. Protein Immobilization on the Surface of Polydimethylsiloxane and Polymethylmethacrylate Microfluidic Devices. Electrophoresis. v. 37, p. 529-535, 2016.
28. J. D. Lopez, A. Dante, R. C. da Silva Allil and M. M. Werneck, "The Influence of Geometric Shape on the Performance of Refractive Index Sensors Based on Plastic Optical Fibers: Simulations and Experimental Assessment," in IEEE Sensors Journal, vol. 23, no. 6, pp. 5803-5809, March 15, 2023. doi: 10.1109/JSEN.2023.3240292